Subsecond total-body imaging using ultrasensitive positron emission tomography

Xuezhu Zhang[a,1], Simon R. Cherry[a,b], Zhaoheng Xie[a], Hongcheng Shi[c], Ramsey D. Badawi[a,b], and Jinyi Qi[a,1]

[a]Department of Biomedical Engineering, University of California, Davis, CA 95616; [b]Department of Radiology, University of California Davis Medical Center, Sacramento, CA 95817; and [c]Department of Nuclear Medicine, Zhongshan Hospital Fudan University, 200032 Shanghai, China

Edited by John A. Rogers, Northwestern University, Evanston, IL, and approved December 31, 2019 (received for review October 4, 2019)

A 194-cm-long total-body positron emission tomography/computed tomography (PET/CT) scanner (uEXPLORER), has been constructed to offer a transformative platform for human radiotracer imaging in clinical research and healthcare. Its total-body coverage and exceptional sensitivity provide opportunities for innovative studies of physiology, biochemistry, and pharmacology. The objective of this study is to develop a method to perform ultrahigh (100 ms) temporal resolution dynamic PET imaging by combining advanced dynamic image reconstruction paradigms with the uEXPLORER scanner. We aim to capture the fast dynamics of initial radiotracer distribution, as well as cardiac motion, in the human body. The results show that we can visualize radiotracer transport in the body on timescales of 100 ms and obtain motion-frozen images with superior image quality compared to conventional methods. The proposed method has applications in studying fast tracer dynamics, such as blood flow and the dynamic response to neural modulation, as well as performing real-time motion tracking (e.g., cardiac and respiratory motion, and gross body motion) without any external monitoring device (e.g., electrocardiogram, breathing belt, or optical trackers).

positron emission tomography | ultrahigh temporal resolution | fast tracer imaging | real-time motion capture

Positron emission tomography (PET) is the most sensitive imaging modality for tracing biomedical processes in vivo (1). It has been widely applied in clinical diagnosis and research areas that span physiology, biochemistry, and pharmacology. One unique feature of PET is the simultaneous acquisition of all projection data such that its intrinsic temporal resolution is not limited by physical (such as gantry rotation in X-ray computed tomography [CT]) or electronic (such as pulse sequences in magnetic resonance imaging [MRI]) scanning. Rather, the practical temporal resolution of a PET scanner is limited by the counting statistics of coincident photon detection (2). Due to the limitations in the amount of activity that can be injected, PET data typically have low counting statistics.

To overcome this limitation, the EXPLORER (EXtreme Performance LOng axial REsearch scanneR) consortium has built a 194-cm-long PET/CT scanner (uEXPLORER) (3), which is a three-dimensional medical imaging device that can cover the entire human body at once. It allows simultaneous dynamic imaging of multiple organs with dramatically increased sensitivity. With this benefit, we aim to push the limit of the temporal resolution of dynamic PET by combining an innovative image reconstruction method (kernel expectation maximization [EM]) (4) with this ultrasensitive high-performance scanner. High temporal resolution PET is useful for studying blood flow, transit times, and fast radiotracer dynamics. It can also be used to freeze subject motion, either physiological (such as cardiac and respiratory motion) or involuntary body motion, thereby improving the effective spatial resolution of reconstructed images. The cardiac and respiratory motion captured in dynamic PET images can also provide information for assessing the biomechanical properties of the organ of interest.

In this work, we develop a method to perform ultrahigh temporal resolution dynamic PET imaging and demonstrate its capability using uEXPLORER data. A summary of the uEXPLORER's physical characteristics and reconstruction methods is provided in refs. 5 and 6. A total-body (TB) dynamic scan was performed for 60 min immediately after an intravenous injection of 256 MBq of ^{18}F-fluorodeoxyglucose via a vein in the right leg of a healthy volunteer (60-year-old female), after obtaining informed consent. The study was approved by the Ethics Board of Zhongshan Hospital (Shanghai, China). To demonstrate the high temporal resolution of the proposed method for capturing fast tracer dynamics and real-time cardiac motion, we divided the first-minute data into 100-ms temporal frames and analyzed the reconstructed images. The data are available upon request from the corresponding author.

Results and Discussion

Fig. 1*A* shows maximum intensity projections of the reconstructed dynamic PET images of 10 consecutive 100-ms frames to visualize the cardiac motion. Fig. 1*B* shows 10 selected 100-ms frames, alternating between end-diastolic and end-systolic phases of five cardiac cycles, to show the radiotracer bolus delivery and distribution within the whole body. A full video with 100-ms temporal resolution is available in Movie S1. The total number of detected true coincident events in each temporal frame is less than 1 million. Even at this low count level, the reconstructed images show good image quality. Changes in the cardiac blood pool are well captured by the 100-ms dynamic PET images, with clear delineation of the end-systolic and end-diastolic phases. The flow of the radiotracer as a result of cardiac contraction, which pumps the radiotracer bolus from the left ventricle (LV) to the aorta, from which it is distributed in the arterial tree, can be clearly observed. Fig. 1*C* shows the time–activity curves (TACs) in four regions of interest (ROI) during the first minute after the tracer injection. The four ROIs are drawn in the LV, ascending aorta, descending aorta, and myocardium. Besides the obvious time delay between the three blood curves, they also show a staircase pattern, because new blood enters the LV in the diastolic phase of the cardiac cycle and is pumped into the aorta in the systolic phase of the cardiac cycle. As a result, the radiotracer concentration in the LV only changes in the diastolic phase and remains nearly constant during the

Author contributions: X.Z., S.R.C., R.D.B., and J.Q. designed research; X.Z. performed research; X.Z. and J.Q. analyzed data; X.Z., S.R.C., Z.X., R.D.B., and J.Q. wrote the paper; and H.S. supervised the human scan.

Competing interest statement: University of California, Davis has a research agreement and a revenue sharing agreement with United Imaging Healthcare.

This open access article is distributed under Creative Commons Attribution-NonCommercial-NoDerivatives License 4.0 (CC BY-NC-ND).

[1]To whom correspondence may be addressed. Email: qi@ucdavis.edu or zhang@ucdavis.edu.

This article contains supporting information online at https://www.pnas.org/lookup/suppl/doi:10.1073/pnas.1917379117/-/DCSupplemental.

First published January 21, 2020.

Downloaded at Palestinian Territory, occupied on December 2, 2021

www.manaraa.com

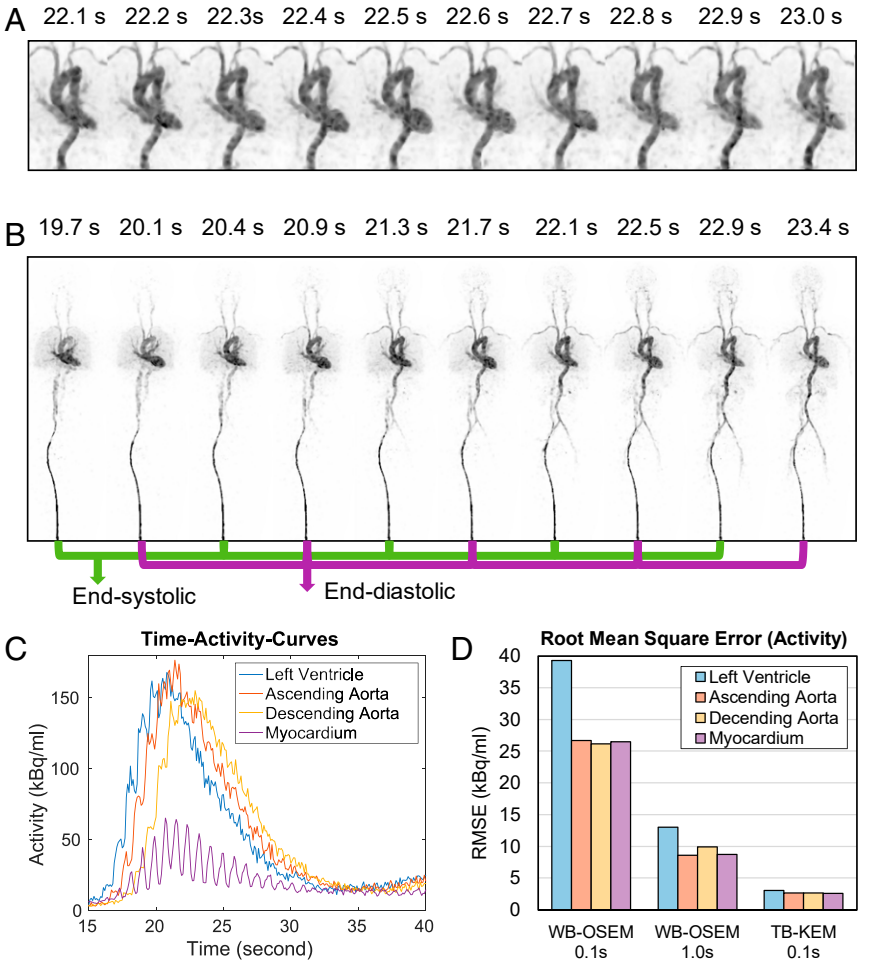

Fig. 1. (*A*) Reconstruction dynamic PET images (maximum intensity projection) of 10 consecutive 100-ms frames from 22 s postinjection. (*B*) Selected dynamic PET images of 100-ms frames alternating between the end-diastolic and end-systolic phases of five cardiac cycles. (*C*) Dynamic TACs from 100-ms frames. (*D*) RMSE of 0.1- and 1-s WB OSEM reconstructions and 0.1-s TB-KEM reconstruction.

systolic phase, whereas the radiotracer concentration in the aorta changes in the systolic phase and remains nearly constant in the diastolic phase. This phenomenon is also evident in the images shown in Fig. 1*B*. The TAC of the descending aorta is lower than those of the LV and ascending aorta, due to increased dispersion of the bolus at that point. The myocardium TAC has a clear cyclical rhythm from the heartbeat, because we used a fixed ROI in which the blood fraction changes with cardiac cycle. All of these observations would not be possible at the lower temporal resolution previously used in dynamic PET imaging. To quantify the improvement over a standard whole-body (WB) scanner, we extracted events corresponding to one detector ring covering the heart region from the uEXPLORER data to mimic a WB scanner with an axial field of view of 24 cm. Using the first 120 s of data as the ground truth, we generated 30 noisy realizations of 0.1- and 1-s scans by resampling the list mode data. The WB data were reconstructed using the standard ordered-subset EM (OSEM) algorithm. Voxel-wise root-mean-squared errors (RMSE) of the reconstructed images were calculated for the four ROIs and plotted in Fig. 1*D*. The RMSE of the proposed 0.1-s TB kernel-EM (TB-KEM) is about 10 times less than the 0.1-s WB scan, and about 3 times less than the 1-s WB scan.

The above results demonstrate that, by combining the kernel-EM reconstruction with the EXPLORER scanner, we can obtain dynamic PET images at 100-ms temporal resolution with good quality. This high temporal resolution tracer imaging technique opens up the opportunity for new applications, such as studying fast pharmacodynamics, using shorter-lived radionuclides (e.g., ^{82}Rb, ^{13}N, and ^{15}O), and performing motion-frozen scans of the heart, lung, and gastrointestinal tract. Although many current clinical imaging systems, such as angiography, CT, MRI, and ultrasound, can locally perform fast imaging and provide specific anatomical or functional information, none of these can generate real-time molecular imaging of physiology and biochemistry process with TB coverage. The quality of the 100-ms images is aided by the high contrast of activity in the vascular system. The optimal temporal sampling and spatial resolution will be different for images of radiotracer activity widely distributed throughout tissues. The image quality can be further improved by incorporating machine learning methods (7).

PET with high temporal resolution also has potential applications in the characterization of normal and abnormal brain function. Although functional MRI can detect changes associated with cerebral blood flow (CBF), our approach has the potential to directly measure the absolute value of CBF and cerebral metabolic rate of oxygen (8). The advantage of CBF as determined with diffusible tracers in PET is that it measures blood flow at the nutrient capillary level (not only in large vessels). During the stimulation, parameters derived within a window of a second may show better correlation with postsynaptic activity and less hemodynamic lag. Moreover, these methods could be

Downloaded at Palestinian Territory, occupied on December 2, 2021
www.manaraa.com

used for localizing neural activity by correlating it with specific neurotransmitter activity (9). Furthermore, without the artifacts induced by cardiac and respiratory motion, ultrafast PET may allow analysis of metabolic processes within atherosclerotic plaques and evaluate their distribution and characteristics throughout the cardiovascular system. Finally, high temporal resolution PET together with the TB coverage allows dynamic tracer studies of brain–heart and brain–gut interactions (10).

In conclusion, we have successfully developed a subsecond TB molecular imaging technique which has applications in real-time tracking of blood flow and motion-frozen imaging of cardiovascular and respiratory functions.

ACKNOWLEDGMENTS. This work was supported, in part, by NIH under Grant R01 CA206187 and the University of California (UC) Davis Innovative Development Award. We acknowledge the contributions of the EXPLORER team members from UC Davis and United Imaging Healthcare.

1. M. E. Phelps, Positron emission tomography provides molecular imaging of biological processes. *Proc. Natl. Acad. Sci. U. S. A.* **97**, 9226–9233 (2000).
2. S. R. Cherry, J. A. Sorenson, M. E. Phelps, *Physics in Nuclear Medicine* (Saunders, 2012).
3. R. D. Badawi *et al.*, First human imaging studies with the explorer total-body PET scanner. *J. Nucl. Med.* **60**, 299–303 (2019).
4. G. Wang, J. Qi, PET image reconstruction using kernel method. *IEEE Trans. Med. Imaging* **34**, 61–71 (2015).
5. X. Zhang *et al.*, Quantitative image reconstruction for total-body PET imaging using the 2-meter long EXPLORER scanner. *Phys. Med. Biol.* **62**, 2465–2485 (2017).
6. X. Zhang *et al.*, Total body dynamic reconstruction and parametric imaging on the uEXPLORER, *J. Nucl. Med.*, 10.2967/jnumed.119.230565 (2019).
7. K. Gong *et al.*, Iterative PET image reconstruction using convolutional neural network representation. *IEEE Trans. Med. Imaging* **38**, 675–685 (2019).
8. N. Kudomi *et al.*, Rapid quantitative measurement of $CMRO_2$ and CBF by dual administration of ^{15}O-labeled oxygen and water during a single PET scan—A validation study and error analysis in anesthetized monkeys. *J. Cereb. Blood Flow Metab.* **25**, 1209–1224 (2005).
9. V. N. Salimpoor, M. Benovoy, K. Larcher, A. Dagher, R. J. Zatorre, Anatomically distinct dopamine release during anticipation and experience of peak emotion to music. *Nat. Neurosci.* **14**, 257–262 (2011).
10. E. A. Mayer, Gut feelings: The emerging biology of gut–brain communication. *Nat. Rev. Neurosci.* **12**, 453–466 (2011).

Downloaded at Palestinian Territory, occupied on December 2, 2021

www.manaraa.com